# Large magnetoelastic effects in paramagnetic stainless steels from first principles

L. Vitos[1,2,3] and B. Johansson[1,2,4]

[1]*Department of Materials Science and Engineering, Applied Materials Physics, Royal Institute of Technology, SE-100 44 Stockholm, Sweden*

[2]*Department of Physics and Materials Science, Division for Materials Theory, Uppsala University, SE-75121 Uppsala, Sweden*

[3]*Research Institute for Solid State Physics and Optics, H-1525 Budapest, P.O. Box 49, Hungary*

[4]*School of Physics and Optoelectronic Technology & College of Advanced Science and Technology, Dalian University of Technology, Dalian 116024, China*

(Received 3 September 2008; revised manuscript received 26 November 2008; published 13 January 2009)

Using first-principles theories, we demonstrate that the elastic properties of substitutional disordered Fe-rich Fe-Cr-Ni alloys (austenitic stainless steels) sensitively depend on their magnetic state. Due to the strong magnetoelastic effects in paramagnetic $Fe_{0.70}Cr_{0.15}Ni_{0.15}$ alloy, the room-temperature magnetism is found to alter the usually dominating chemical effects and give a large anomalous contribution to the temperature dependence of the elastic constants.

DOI: 10.1103/PhysRevB.79.024415 PACS number(s): 75.80.+q, 75.50.Bb, 71.15.Nc, 81.05.Zx

## I. INTRODUCTION

Austenitic stainless steels, the largest subcategory of stainless steels, are substitutionally disordered Fe-Cr-Ni alloys, containing small amount of additional alloying elements (such as Mo, Si, Mn, Al, etc.) and less than 0.4 at. % interstitial carbon. They provide the best corrosion resistance of the stainless group having excellent mechanical properties. The austenitic stainless steels represent the primary choice in nonmagnetic technological applications as well.

At low temperature, the magnetic structure of austenitic steels can be antiferromagnetic, spin glass, or ferromagnetic, depending on Ni and Cr content, whereas at room temperature they are paramagnetic metals.[1] The Curie-Weiss-type susceptibility observed for $Fe_{0.8-n}Cr_cNi_n$ ($c=0.2$ and $0.14<n<0.21$) at temperatures above 26–130 K (Ref. 2) indicates that at room temperature the paramagnetic stainless steels have sizable persisting local magnetic moments. The full austenite phase has the face-centered-cubic (fcc) crystallographic structure of $\gamma$-Fe. In commercial austenitic stainless steels, the fcc phase is stabilized by chemical, magnetic, and thermal effects.

The possible impact of magnetism on the properties of Fe-based engineering materials was pointed out already in the 1950s.[3] Since then, extensive efforts were devoted to reveal the footprint of magnetic transition on the low-temperature properties of steels.[4–8] However, the progress in understanding the role of paramagnetism on the basic properties of austenitic steels at room temperature has remained very scarce. Among the limited number of attempts, we mention our former works,[9,10] where we used the stacking fault energy for identifying the impact of room-temperature spin fluctuations (sf) on the cohesive properties of austenitic steels.

The accurate knowledge of the elastic constants and the atomic-scale phenomena behind their variation promotes the understanding of the fundamental aspects of a wide diversity of properties that the austenitic stainless steels exhibit. In contrast to the stacking fault energies,[9,10] the engineering elastic constants of paramagnetic steels were found to show a relatively weak compositional dependence.[11,12] Here, we investigate the effect of magnetism on the elastic properties of paramagnetic Fe-Cr-Ni alloys. We focus on the Fe15Cr15Ni system containing 15 at. % Cr and 15 at. % Ni, which undergoes a paramagnetic fcc to ferromagnetic body-centered-cubic (bcc) phase transition near 190 K.[7] We demonstrate that in the paramagnetic state, the elastic constants and their composition and temperature dependences are determined by the disordered local magnetic moments present in this family of materials.

The rest of the paper is divided in two main sections and conclusions. Section II presents the first-principles method used in our calculations. The results are presented and discussed in Sec. III. Here, we assess the accuracy of our calculations, show that the room-temperature magnetism alters the usually dominating chemical effects, and investigate the temperature dependence of the elastic constants of paramagnetic Fe-Cr-Ni alloys.

## II. FIRST-PRINCIPLES METHOD

All theoretical results presented here have been obtained using the density-functional theory[13] in combination with the generalized gradient approximation.[14] The Kohn-Sham equations were solved within the exact muffin-tin orbitals (EMTOs) formalism.[15–17] The chemical and magnetic disorder in Fe-Cr-Ni alloys was treated within the coherent-potential approximation (CPA).[18,19]

Ordering effects in austenitic stainless steels were studied among many others by Cenedese *et al.*[20] These authors found that the short-range order parameters in Fe21Cr23Ni are below ~0.15 (0 corresponds to totally random, whereas ±1 to ordered and segregated cases, respectively) indicating a small correlation between alloying elements. Furthermore, it was found that the correlation between Cr and Ni is short ranged, there is a weak correlation between Fe and Cr and no correlation between Fe and Ni. Later, it was shown that the short-range ordering in Fe-Cr-Ni system increases with Ni amount.[21] Taking into account the above findings and the fact that the austenitic stainless steels considered in the

 

TABLE I. Theoretical equilibrium atomic radius ($w_0$), local magnetic moment ($\mu_0$), bulk modulus ($B$), and single-crystal elastic constants ($c_{ij}$) of PM, FM, and NM fcc Fe15Cr15Ni alloys. The present results are compared to the room-temperature experimental data (expt.) for the paramagnetic alloy (Ref. 7) NM* stands for nonmagnetic results obtained at the equilibrium volume of the paramagnetic phase. The numbers in parenthesis are the relative deviations (in %) between theory and experiment.

| | $w_0$ (Bohr) | $\mu_0$ ($\mu_B$) | $B$ (GPa) | $c_{11}$ (GPa) | $c_{12}$ (GPa) | $c'$ (GPa) | $c_{44}$ (GPa) |
|---|---|---|---|---|---|---|---|
| PM | 2.660 | 1.63 | 162.23 | 203.86 | 141.42 | 31.22 | 133.20 |
| | (0.4) | | (1.1) | (−2.5) | (4.0) | (−14.5) | (2.5) |
| FM | 2.698 | 1.30 | 177.36 | 175.04 | 178.52 | −1.74 | 89.50 |
| | (1.8) | | (10.5) | (−16.3) | (31.3) | (−104.8) | (−31.2) |
| NM | 2.612 | | 246.22 | 334.42 | 202.12 | 66.12 | 195.16 |
| | (−1.4) | | (53.4) | (60.0) | (48.6) | (81.2) | (50.1) |
| NM* | 2.660 | | 200.06 | 276.94 | 161.62 | 57.66 | 162.12 |
| | | | (24.6) | (32.5) | (18.8) | (58.0) | (24.7) |
| Expt. | 2.65 | | 159–162 | 207–211 | 135–137 | 35–38 | 130 |

present work are built around 15% Cr and 15% Ni, one can assume that the short-range order effects play a small role in the energetics of these materials. Therefore, the employed single-site CPA represents an appropriate tool to compute the composition and magnetic-moment dependence of the total energy.

The paramagnetic state of the ternary $Fe_{1-c-n}Cr_cNi_n$ alloy was modeled by a four component alloy $(Fe^{\uparrow}_{0.5}Fe^{\downarrow}_{0.5})_{100-c-n}Cr_cNi_n$ with randomly distributed up ($\uparrow$) and down ($\downarrow$) magnetic moments on Fe atoms. This disordered local magnetic-moment picture correctly accounts for the loss of the net magnetic moment above the transition temperature.[22–25] In the present calculations, we neglected the magnetic moments on Cr and Ni. These moments appear only as a result of thermal spin fluctuations and remain small at room temperature.[9,16] However, since Fe forms 70% of the alloy, we expect that neglecting the Cr and Ni moments introduces only small errors.

There are three independent cubic elastic constants: $c_{11}$, $c_{12}$, and $c_{44}$. For each alloy, the theoretical equilibrium atomic radius $w_0$ and the bulk modulus $B=(c_{11}+2c_{12})/3$ were determined from an exponential Morse-type function[26] fitted to the *ab initio* total energies of fcc structure for 11 different atomic radii $w$. In order to calculate the two cubic shear moduli $c'=(c_{11}-c_{12})/2$ and $c_{44}$, we used volume conserving orthorhombic and monoclinic deformations, as described, e.g., in Ref. 27.

The electronic structure was calculated by solving the scalar relativistic Kohn-Sham equations for the valence electrons and the EMTO basis set included $s$, $p$, $d$, $f$ orbitals. In the irreducible wedge of the Brillouin zones, we used 1300–1700 $k$ points, depending on the particular distortion.

## III. RESULTS

### A. Assessing the accuracy

Since no independent theoretical results are available for Fe15Cr15Ni, we use the recent experimental data[7] to establish the accuracy of the present approach for the elastic constant (Table I). We find 3.0% mean absolute relative deviation between the theoretical and experimental single-crystal elastic constants for paramagnetic (PM) Fe15Cr15Ni alloy. As a matter of fact, this error is much smaller than ~13% obtained for ferromagnetic bcc Fe[28] or that obtained for nonmagnetic transition metals.[29] The conspicuously better accuracy achieved for Fe-Cr-Ni compared to Fe might be due to the fact that our approach gives a highly accurate equation of state (EOS) for paramagnetic Fe-Cr-Ni: the relative errors in the equilibrium atomic radius and bulk modulus being 0.4% and 1.1%, respectively. The good parallelism between the theoretical and experimental results indicates that the EMTO method along with the employed approximation is suitable to reveal the atomic-scale phenomena behind the elastic properties of austenitic steels.

### B. Magnetic versus chemical effects

In Table I, we also list the results obtained for ferromagnetic (FM) and nonmagnetic (NM) Fe15Cr15Ni alloys. Both of these EOSs are in poor agreement with the experiment. This is reflected in the large mean absolute errors in $c_{ij}$: ~26% for FM and ~53% for NM. In fact, fcc Fe15Cr15Ni is calculated to be mechanically unstable in the FM state. Repeating the NM calculation at PM volume decreases the mean error to ~26%, but this is still well above the one obtained for the PM state.

The fact that the elastic constants of Fe15Cr15Ni depend so sensitively on the magnetic state is not surprising: similar effects are seen also in elemental Fe. More important is that different magnetic states yield very different alloying effects on the single-crystal elastic constants. The results in Table II have been obtained by computing the elastic constants for Fe13Cr15Ni and Fe17Cr15Ni, as well for Fe15Cr13Ni and Fe15Cr17Ni, and taking the numerical derivatives against Cr ($c$) or Ni ($n$) concentration.

Except $c_{12}$ versus $c$ and $c_{44}$ versus $n$, the two sets of results from Table II differ significantly. We find that mag-

TABLE II. Calculated alloying effects on the elastic constants of paramagnetic Fe15Cr15Ni random alloy. The alloying effects are given per concentration of Cr $[(1/c_{ij})(\delta c_{ij}/\delta c)]$ or Ni $[(1/c_{ij})(\delta c_{ij}/\delta n)]$.

| | $\frac{1}{c_{11}}\frac{\delta c_{11}}{\delta c}$ | $\frac{1}{c_{12}}\frac{\delta c_{12}}{\delta c}$ | $\frac{1}{c_{44}}\frac{\delta c_{44}}{\delta c}$ | $\frac{1}{c_{11}}\frac{\delta c_{11}}{\delta n}$ | $\frac{1}{c_{12}}\frac{\delta c_{12}}{\delta n}$ | $\frac{1}{c_{44}}\frac{\delta c_{44}}{\delta n}$ |
|---|---|---|---|---|---|---|
| PM | 0.41 | 0.74 | −0.07 | 0.10 | 0.33 | −0.24 |
| NM | −0.37 | 0.46 | −1.12 | −0.39 | −0.31 | −0.36 |

netism significantly alters the alloying effects obtained for the NM phase. It is clear that no accurate modeling of the dynamical properties of paramagnetic steels as a function of chemical composition is possible without properly accounting for the disordered local magnetic moments.

Before closing this section, we would like to emphasize that the present theoretical data from Table II should not be compared with the experimental values from Ref. 7. First of all, our theoretical coefficients refer to 0 K, whereas those from Ref. 7 are given for the room temperature. Due to the large temperature factor in $c_{ij}(T)$ (see Sec. III D), such comparison is meaningful only if the two sets of data are obtained under similar conditions. More importantly, a detailed investigation of the experimental elastic constant database (Table III in Ref. 7) shows that the experimental coefficients listed in Table IV (Ref. 7) are not reliable. Because of that, today we consider it premature to make any direct comparison between the *ab initio* and experimental coefficients for the compositional dependence of the elastic constants of paramagnetic austenitic stainless steels.

### C. Magnetoelastic coupling

The cubic elastic constants computed as a function of local moments on the Fe atoms ($\mu$) can be used to illustrate the impact of magnetism on the elastic properties of Fe15Cr15Ni alloy (Fig. 1). In these calculations, we used the PM equilibrium volume and fixed the Fe local magnetic moments during the lattice distortion. For reference, in Fig. 1 the fully self-consistent results are also shown (separate symbols). The deviation between these values and those obtained within the spin-constrained calculation for $\mu_0=1.63\mu_B$ gives further evidence for the large magnetostructural coupling in austenitic steels.[9]

From a polynomial fit to the data from Fig. 1, for the slopes of the elastic constants versus magnetic moment we obtain $\delta c'/\delta\mu \approx -22.5$ GPa/$\mu_B$ and $\delta c_{44}/\delta\mu \approx -19.5$ GPa/$\mu_B$. Hence, $0.1\mu_B$ change in the local magnetic moment results in ~2 GPa change in the elastic constants, representing ~6% for $c'$ and ~2% for $c_{44}$. This is an important effect, especially taking into account that we are dealing with a system well above its magnetic transition temperature. We suggest that by manipulating the magnetism, e.g., via chemical composition, chemical ordering, external field, or temperature, one is able to tailor the thermoelastic properties of austenitic stainless steels. Here we demonstrate this effect through the temperature dependence of $c_{ij}(T)$.

### D. Temperature dependence of $c_{ij}(T)$

Recently, Teklu *et al.*,[7] using resonant ultrasound spectroscopy and pulse-echo superposition techniques, measured

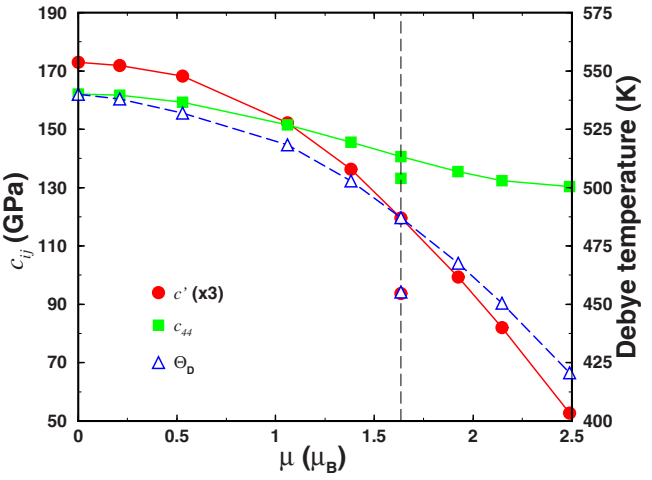


FIG. 1. (Color online) Left axis: single-crystal elastic constants of paramagnetic Fe15Cr15Ni alloy as a function of the local magnetic moment on the Fe atoms (red circles and green squares connected by solid lines). Note that $c'$ has been multiplied by three in order to match its scale to that of $c_{44}$. Right axis: Debye temperature of paramagnetic Fe15Cr15Ni alloy as a function of the local magnetic moment on the Fe atoms (blue triangles connected by dashed line). Shown are also the floating spin results obtained at the equilibrium magnetic moment $\mu_0=1.63\mu_B$ (separate circle, square, and triangle). All calculations were performed at PM volume (corresponding to $w_0=2.66$ bohr).

the elastic constants for single crystals of Fe15Cr15Ni alloy as a function of temperature. They found that above the magnetic transition temperature $(\delta c'/\delta T)/c' \approx -6\times10^{-4}$ 1/K and $(\delta c_{44}/\delta T)/c_{44} \approx -4\times10^{-4}$ 1/K. The temperature factor for $c'$ significantly exceeds those obtained for the alloying elements, which suggests that the elastic properties of paramagnetic steels exhibit anomalous temperature dependence.

To compute the temperature-dependent elastic constants, we adopt the approach from Ref. 30. According to that, we separate the constant volume and constant-temperature contributions to $C(T)$ ($C$ stand for $c'$ or $c_{44}$) as

$$\Delta C(T) \equiv C(T,V) - C(T_0,V_0)$$
$$= C(T,V) - C(T,V_0) + C(T,V_0) - C(T_0,V_0), \quad (1)$$

where $V$ and $V_0$ are the volumes at $T$ and $T_0$, respectively. $T_0$ is the reference temperature (e.g., 0 K). The constant temperature or the anharmonic (ah) part of $\Delta C(T)$, i.e., $C(T,V) - C(T,V_0)$, is calculated from the volume expansion as described in Sec. III D 1. The constant volume contribution to $\Delta C(T)$, i.e., $C(T,V_0) - C(T_0,V_0)$, is obtained from explicit density-functional calculations carried out at fixed volume, as described in Secs. III D 2 and III D 3.

#### 1. Anharmonic effects

The thermal expansion caused by anharmonicity gives a monotonically decreasing $c_{ij}(T)$ with increasing temperature.[31] This effect can be estimated from the volume dependence of the elastic constants as $(\delta c_{ij}/\delta T)_{\rm ah} \approx \delta c_{ij}/\delta w \times \delta w/\delta T = \delta c_{ij}/\delta w \times \alpha_{\rm aust} w_0$. For the linear thermal-expansion coefficient of austenitic steels ($\alpha_{\rm aust}$), we use the

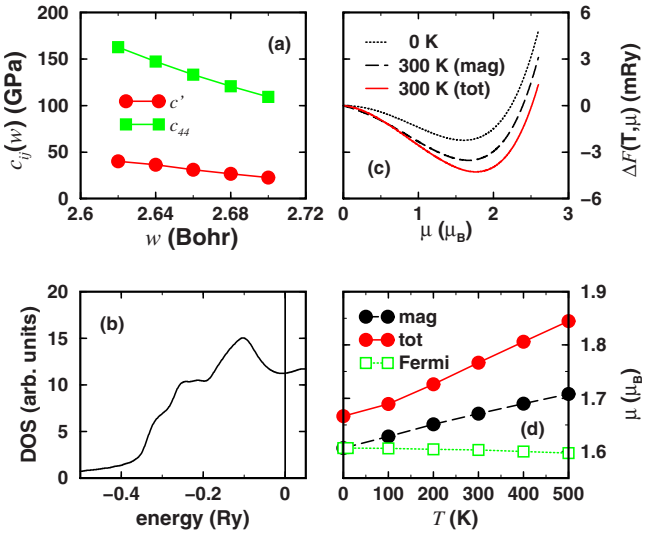


FIG. 2. (Color online) Panel (a): volume dependence of $c'$ (red circles) and $c_{44}$ (green squares) calculated for PM Fe15Cr15Ni. Panel (b): total density of states (in arbitrary units) for PM Fe15Cr15Ni. The vertical line marks the Fermi level. Panel (c): free energy as a function of the local magnetic moment on the Fe atoms for 0 K (black dotted line) and 300 K (red solid line). The additional effect of the lattice vibration is illustrated by the free energy obtained merely from the internal energy and magnetic entropy for 300 K (black dashed line). Panel (d): theoretical magnetic moments (red solid line) versus temperature. Results obtained without lattice vibrations are also plotted (black dashed line). Open squares show the effect of Fermi-Dirac distribution on the local magnetic moments.

average value of $17.3\times10^{-6}$ 1/K. The present $c'(w)$ and $c_{44}(w)$ functions for paramagnetic Fe15Cr15Ni alloy are shown in Fig. 2(a). From these data, near the PM equilibrium volume we obtain $\delta c'/\delta w\approx-224.05$ GPa/Bohr and $\delta c_{44}/\delta w\approx-664.74$ GPa/bohr. For comparison, in nonmagnetic alloy (not shown), the above slopes are −160.2 GPa/bohr and −638.3 GPa/bohr, respectively.

The present values for $(\delta c_{ij}/\delta T)_{\text{a.h.}}$ are listed in Table III for both PM and NM states. When compared to the experimental data (last column in Table III), we find that anharmonicity in PM steels can only account up to 48% and 65% of the measured temperature dependence of $c'$ and $c_{44}$, respectively. Note that in the NM case, this discrepancy is significantly larger for $c'$. Therefore, further mechanisms are needed to explain the reported anomalous behavior of $c_{ij}(T)$ in austenitic steels.[7]

### 2. Fermi-Dirac distribution

Superimposed to the above normal behavior, in some solids (e.g., Nb or Pd) a strong irregular temperature dependence of the elastic constants might appear as a result of the Fermi-Dirac distribution.[30,31] In paramagnetic steel, however, the average density of states shows no peculiar structure near the Fermi level [Fig. 2(b)], ruling out the presence of such anomalous terms in $\delta c_{ij}/\delta T$. On the other hand, the strong magnetic-moment dependence of $c_{ij}$ (Fig. 1) indicates that magnetism might be responsible for the observed large $\delta c_{ij}/\delta T$.

TABLE III. Room-temperature theoretical (present results) and experimental (Ref. 7) values for the temperature derivatives of the cubic elastic constants (in units of $10^{-2}\times$GPa/K) for Fe15Cr15Ni alloy in the paramagnetic (PM) and nonmagnetic (NM) states (for notations see the text).

| | $(\frac{\delta c_{ij}}{\delta T})_{\text{ah}}$ | $(\frac{\delta c_{ij}}{\delta T})_{\text{sf}}$ | $(\frac{\delta c_{ij}}{\delta T})_{\text{tot}}$ | $(\frac{\delta c_{ij}}{\delta T})_{\text{expt.}}$ |
|---|---|---|---|---|
| $c'$(PM) | −1.0 | −0.9 | −1.9 | −2.1 |
| $c_{44}$(PM) | −3.2 | −0.8 | −4.0 | −4.9 |
| $c'$(NM) | −0.7 | | −0.7 | −2.1 |
| $c_{44}$(NM) | −2.9 | | −2.9 | −4.9 |

### 3. Spin-fluctuation effects

We approximate the explicit electron structure-dependent terms in $\delta c_{ij}/\delta T$ by the longitudinal spin-fluctuation contribution, viz. $(\delta c_{ij}/\delta T)_{\text{sf}}\approx\delta c_{ij}/\delta\mu\times\delta\mu/\delta T$, where $\delta c_{ij}/\delta\mu$ is given in Fig. 1 and $\delta\mu/\delta T$ describes the temperature dependence of the average local magnetic moments on Fe. The latter can be determined from the total free energy $F(T,\mu)\approx E(\mu)-TS_{\text{mag}}(\mu)+F_{\text{ph}}(T,\mu)$, where $E(\mu)$ is the internal energy. Self-consistent test calculations carried out for Fermi temperatures up to 500 K show that the Fermi-Dirac distribution decreases the size in the local magnetic moment, in line with Ref. 25. Nevertheless, in paramagnetic Fe15Cr15Ni this effect in absolute value is less than $0.2\times10^{-4}\mu_B$/K [Fig. 2(d), open squares], which is negligible compared to the other entropy effects (see below). Because of that, in the present study the one-electron excitations were omitted. Accordingly, the temperature effects in $F(T,\mu)$ enter only through the magnetic entropy term $TS_{\text{mag}}(\mu)$ and the phonon free energy $F_{\text{ph}}(T,\mu)$. The former was approximated by the mean-field expression $k_B\log(\mu+1)$ ($k_B$ is the Boltzmann constant), whereas the latter was obtained within the Debye model (see, e.g., Ref. 32).

The magnetic entropy always favors larger average local magnetic moments. In paramagnetic steels, the vibrational free energy is also expected to increase the average local magnetic moments. This is seen from the Debye temperature plotted as a function of magnetic moment (Fig. 1, right axis): the fcc lattice becomes softer with increasing local magnetic moments. Near the equilibrium magnetic moment, we have $\delta\Theta_D/\delta\mu\approx-62.06$ K/$\mu_B$. Such a big change in the elastic constant Debye temperature can easily alter the local magnetic moments already at room temperature.

The free energy for the paramagnetic Fe15Cr15Ni alloy is plotted in Fig. 2(c) as a function magnetic moment for 0 and 300 K (all calculated at PM volume). We find that the shallow minimum near $1.63\mu_B$ for 0 K is shifted to $\sim1.77\mu_B$ at 300 K. The corresponding $\mu(T)$ curve obtained from the minimum of the free energies for $T=0,100,200,\ldots,500$ K, is plotted in Fig. 2(d) (solid line). Near the room temperature, the average local magnetic moments on the Fe atoms are obtained to increase as $\delta\mu/\delta T\approx4\times10^{-4}\mu_B$/K. We mention that the slope of the magnetic moment obtained merely from internal energy and magnetic entropy [Figs. 2(c) and 2(d), dashed lines] would be slightly less than half of the above total slope. Using $\delta\mu/\delta T$ and the slopes for $c_{ij}$ versus

$\mu$ (Fig. 1), we get the temperature factors for $c_{ij}$ due to longitudinal magnetic fluctuations (Table III). The total temperature derivatives $(\delta c_{ij}/\delta T)_{\text{tot}}$ are then obtained as the sum of the ah and spin sf contributions. These theoretical derivatives are in good agreement with the experimental data: the relative deviations being 9% and 18% for $c'$ and $c_{44}$, respectively.

## IV. CONCLUSIONS

Using the EMTO method, we have modeled the paramagnetic Fe-Cr-Ni system and have shown that the disordered local magnetic moments have an unexpectedly large impact on the elastic properties. For instance, identifying the total magnetic contribution to the temperature derivatives of the elastic constants with the difference between results obtained for PM and NM states (Table III), we find that magnetism can account for 63% of $(\delta c'/\delta T)_{\text{tot}}$ and 28% for $(\delta c_{44}/\delta T)_{\text{tot}}$. Hence, the magnetic effects are especially important for the tetragonal elastic constant of paramagnetic stainless steels.

Magnetoelastic phenomena in magnetic materials and, in particular, in alloy steels have been known for a long time.[3–8] However, the magnetic effects on the elastic constants of magnetic materials in their paramagnetic state have been less well documented. Here, using first-principles computational methods, we have investigated the atomic-scale effects behind the elastic properties of paramagnetic Fe-Cr-Ni alloys. We have demonstrated that in this important class of "nonmagnetic" engineering materials, magnetism gives a major contribution to the elastic properties and to their chemical composition and temperature dependences.

## ACKNOWLEDGMENTS

The Swedish Research Council, the Swedish Foundation for Strategic Research, and the Hungarian Scientific Research Fund (Grants No. T046773 and No. T048827) are acknowledged for financial support.

[1] A. K. Majumdar and P. v. Blanckenhagen, Phys. Rev. B **29**, 4079 (1984).
[2] T. K. Nath, N. Sudhakar, E. J. McNiff, and A. K. Majumdar, Phys. Rev. B **55**, 12389 (1997).
[3] C. Zener, Trans. AIME **203**, 619 (1955); J. Met. **7**, 619 (1955).
[4] See, e.g., W. F. Weston, H. M. Ledbetter and E. R. Naimon, Mater. Sci. Eng. **20**, 185 (1975).
[5] H. M. Ledbetter and E. W. Collings, Mater. Sci. Eng. **68**, 233 (1984–1985).
[6] H. M. Ledbetter and S. Kim, J. Mater. Sci. **23**, 2129 (1988) and references therein.
[7] A. Teklu, H. Ledbetter, S. Kim, L. A. Boatner, M. McGuire, and V. Keppens, Metall. Mater. Trans. A **35**, 3149 (2004).
[8] E. F. Wassermann, in *Ferromagnetic Materials*, edited by K. H. J. Buschow (Elsevier, New York, 1990), Vol. 5, pp. 237–322.
[9] L. Vitos, P. A. Korzhavyi, and B. Johansson, Phys. Rev. Lett. **96**, 117210 (2006).
[10] L. Vitos, J.-O. Nilsson, and B. Johansson, Acta Mater. **54**, 3821 (2006).
[11] L. Vitos, P. A. Korzhavyi, and B. Johansson, Phys. Rev. Lett. **88**, 155501 (2002).
[12] L. Vitos, P. A. Korzhavyi, and B. Johansson, Nature Mater. **2**, 25 (2003).
[13] P. Hohenberg and W. Kohn, Phys. Rev. **136**, B864 (1964); W. Kohn and L. J. Sham, *ibid.* **140**, A1133 (1965).
[14] J. P. Perdew, K. Burke, and M. Ernzerhof, Phys. Rev. Lett. **77**, 3865 (1996).
[15] L. Vitos, Phys. Rev. B **64**, 014107, (2001).
[16] L. Vitos, *Computational Quantum Mechanics for Materials Engineers: The EMTO Method and Applications, Engineering Materials and Processes Series* (Springer-Verlag, London, 2007).
[17] O. K. Andersen, O. Jepsen, and G. Krier, in *Lectures on Methods of Electronic Structure Calculations*, edited by V. Kumar, O. K. Andersen, and A. Mookerjee (World Scientific Publishing Co., Singapore, 1994), pp. 63–124.
[18] P. Soven, Phys. Rev. **156**, 809 (1967); B. L. Gyorffy, Phys. Rev. B **5**, 2382 (1972).
[19] L. Vitos, I. A. Abrikosov, and B. Johansson, Phys. Rev. Lett. **87**, 156401 (2001).
[20] P. Cenedese, F. Bley, and S. Lefebvre, Acta Crystallogr., Sect. A: Found. Crystallogr. **40**, 228 (1984).
[21] G. S. Was, T. R. Allen, J. T. Busby, J. Gan, D. Damcott, D. Carter, M. Atzmon, and E. A. Kenik, J. Nucl. Mater. **270**, 96 (1999) and references therein.
[22] T. Oguchi, K. Terakura, N. Hamada, J. Phys. F: Met. Phys. **13**, 145 (1983).
[23] B. L. Gyorffy, A. J. Pindor, J. Staunton, G. M. Stocks, and H. Winter, J. Phys. F: Met. Phys. **15**, 1337 (1985).
[24] F. J. Pinski, J. Staunton, B. L. Györffy, D. D. Johnson, and G. M. Stocks, Phys. Rev. Lett. **56**, 2096 (1986).
[25] A. J. Pindor, J. Staunton, G. M. Stocks, and H. Winter, J. Phys. F: Met. Phys. **13**, 979 (1983).
[26] V. L. Moruzzi, J. F. Janak, and K. Schwarz, Phys. Rev. B **37**, 790 (1988).
[27] A. Taga, L. Vitos, B. Johansson, and G. Grimvall, Phys. Rev. B **71**, 014201 (2005).
[28] Y. Guo and H. H. Wang, Chin. J. Phys. **38**, 949 (2000).
[29] P. Söderlind, O. Eriksson, J. M. Wills, and A. M. Boring, Phys. Rev. B **48**, 5844 (1993).
[30] L. Huang, L. Vitos, S. K. Kwon, B. Johansson, and R. Ahuja, Phys. Rev. B **73**, 104203 (2006).
[31] G. Grimvall, *Thermophysical Properties of Materials* (North-Holland, Amsterdam, 1999).
[32] K. Kádas, L. Vitos, B. Johansson and J. Kollár, Phys. Rev. B **75**, 035132 (2007).